Computers and Concrete, *Vol. 22, No. 6 (2018) 527-538*
DOI: https://doi.org/10.12989/cac.2018.22.6.527

Local buckling of reinforcing steel bars in RC members under compression forces

Giovanni Minafò*

Department of Civil, Environmental, Aerospace and Materials Engineering - DICAM, University of Palermo, Viale delle Scienze Ed.8, 90128 Palermo, Italy

(Received October 2, 2018, Revised December 13, 2018, Accepted December 15, 2018)

Abstract. Buckling of longitudinal bars is a brittle failure mechanism, often recorded in reinforced concrete (RC) structures after an earthquake. Studies in the literature highlights that it often occurs when steel is in the post elastic range, by inducing a modification of the engineered stress-strain law of steel in compression. A proper evaluation of this effect is of fundamental importance for correctly evaluating capacity and ductility of structures. Significant errors can be obtained in terms of ultimate bending moment and curvature ductility of an RC section if these effects are not accounted, as well as incorrect evaluations are achieved by non-linear static analyses. This paper presents a numerical investigation aiming to evaluate the engineered stress-strain law of reinforcing steel in compression, including second order effects. Non-linear FE analyses are performed under the assumption of local buckling. A role of key parameters is evaluated, making difference between steel with strain hardening or with perfectly plastic behaviour. Comparisons with experimental data available in the literature confirm the accuracy of the achieved results and make it possible to formulate recommendations for design purposes. Finally, comparisons are made with analytical formulations available in the literature and based on obtained results, a modification of the stress-strain law model of Dhakal and Maekawa (2002) is proposed for fitting the numerical predictions.

Keywords: buckling; steel; finite elements; reinforcement; stress-strain law

1. Introduction

Second order effects in reinforcing steel bars of RC members are usually observed as failure mechanisms in existing structures after strong ground motions. Their probability is related to the loading conditions experienced by the columns in framed structures during seismic actions. In particular, if the member sustains great shortenings, or alternate tensile-compressive axial force values, the cover can be spalled off and the longitudinal steel reinforcements are free to buckle outside the section (Bechtoula *et al*. 2005). Moreover, the inner core tends to expand laterally and it exerts a pressure on the bars, which is subjected to a combined effect of axial force and biaxial bending moment. These conditions induce buckling in the reinforcement, which generally occurs when the bar is in the post-elastic range.

In fact, elastic buckling is reached only when the stirrups' pitch is very large. In particular, this condition occurs when the bar's geometrical slenderness λ_0, calculated by assuming that the bar is clamped inside the pitch, exceeds the limit Eulerian slenderness λ_e. This last is calculated as

$$\lambda_e = \pi\sqrt{\frac{E_s}{f_y}} \tag{1}$$

∗Corresponding author, Assistant Professor
E-mail: giovanni.minafo@unipa.it

where E_s is the Young modulus of steel and f_y is the yield stress.

Differently, for lower values of λ_0, plastic buckling occurs and critical load is achieved after yielding. Generally, distinction is made between local or global buckling (Massone and Moroder 2009) depending if the critical length is equal to the stirrup's pitch or it involves more stirrups. Several studies in the literature investigated the evaluation of the critical length of reinforcing bars and provided indications for its estimation and a recent review on the state of the art can be found in Minafò and Papia (2017). Literature studies demonstrated also that when global buckling occurs a sudden loss of the load-carrying capacity can be observed due to sudden stirrups' failure and to the loss of confinement effects (Campione and Minafò 2010, Yön and Calay 2014).

However, also if the critical length is equal to the stirrups' pitch, it was observed experimentally that inelastic buckling induces a substantial modification of the engineered stress-strain law in the compression of the steel bar (Mander 1983, Monti and Nuti 1992, Mander *et al*. 1994, Bayrak and Sheik 2001), by inducing a softening branch, with slope depending on the slenderness of the bar.

One of the first introductory study on the subject was that of Gomes and Appleton (1997), who assessed steel buckling conditions by adopting the equilibrium of a rigid-plastic mechanism of the buckled bar. On that basis, the researchers proposed a modification of the Menegotto-Pinto cyclic stress-strain steel relationship, which is nowadays included in different simulation codes, such as OpenSees. Monti and Nuti (1992) developed a rule-based plasticity

ISSN: 1598-8198 (Print), 1598-818X (Online)

hardening model, modified for buckling. The model considers kinematic, isotropic, memory, and saturation hardening rules and it requires calculation of some characteristic points for determining an explicit stress-strain relation. More recently, Zong *et al*. (2013) developed a cyclic model for reinforcing steel that included the effects of buckling and low-cycle fatigue. In particular, they developed a simplified "beam-on-springs" models in order to generate average stress-strain relations for reinforcing bars in RC columns with circular crosss-sections. Can Girgin *et al*. (2018) carried out a numerical implementation for dynamic non-linear simulations via a fiber based computational model of RC columns. The model uses force-based elements with a fiber sectional model and it considers a phenomenological stress-strain law of steel rebars capable of simulating inelastic buckling and rupture due to low-cycle fatigue. Fiber elements proved to be effective for modeling different non-linear problems, but when analyzing local buckling of steel bars, the mesh dependence of the model can induce strain localization problems (Shirmohammadi and Esmaeily 2016). For this reason, Kolwankar *et al*. (2017) recently presented a uniaxial nonlocal formulation for a steel bar subjected to buckling-induced localization in compression. The localization phenomenon is taken into account by an explicit length scale, and obtained strain distributions within the localized zone that were compared with those obtained from continuum FE simulations.

All of these models tend to be either computationally expensive or too difficult for direct implementation in design applications. For this reason, some simplified models were developed in the literature, aiming to define of a simplified law, useful for monotonic static non-linear analyses or for a straightforward evaluation of buckling effects on the compressive behaviour of reinforcing steel, such as the law proposed by Dhakal and Maekawa (2002) or that presented in Urmson and Mander (2002). This paper presents a numerical-analytical investigation aiming to evaluate the engineered stress-strain law of reinforcing steel in compression, taking into account buckling effects. Under the assumption of monotonic load, existing literature models for calculating the stress-strain law for steel in compression are examined, and achievable results are compared. On the basis of results obtained by these model, a numerical investigation is performed. The bar is modelled with brick elements, under assumption of critical length equal to the stirrup's pitch (local buckling). Non-linear FE analyses are performed, making difference between steel with strain hardening branch and perfectly plastic behaviour. Comparisons with experimental data available in the literature confirmed the reliability of achieved results and made it possible to state some conclusions, which can be useful for design purposes. Finally, comparisons are made with analytical formulations available in the literature and based on obtained results, a modification of the stress-strain law model of Dhakal and Maekawa (2002) is proposed, for fitting numerical models. The proposed modification allows the definition of an analytical law consistent with FE analyses and experimental data available in the literature and it could be useful for modelling steel rebars for static non-linear analyses of RC structures.

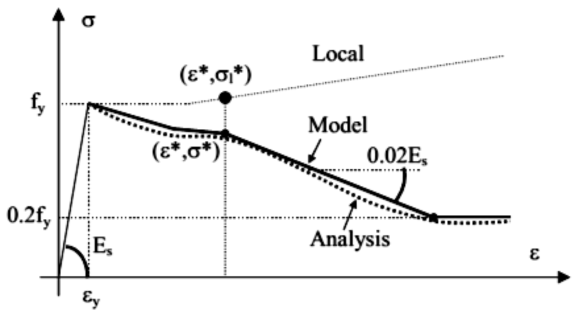

Fig. 1 Model of Dhakal and Maekawa (2002)

2. Existing models for predicting the monotonic compressive response of reinforcing steel

2.1 Model of Dhakal and Maekawa (2002)

Dhakal and Maekawa (2002) performed several numerical analyses and compared results with those derived from experiments. They found that the response was a function of the coefficient FLD, defined as

$$\mathrm{FLD} = \frac{\mathrm{L}}{\mathrm{d_b}}\sqrt{\mathrm{f_y}/100} \tag{2}$$

where f_y is the yield stress, L is the length of the bar, d_b is the diameter of the bar.

Eq. (2) expressed that second order effects in the compressive response of a steel bar depend not only on the geometrical slenderness but also on the mechanical features of the bar, such as the yield stress.

In fact, Dhakal and Maekawa (2002) demonstrated that the trend of the stress-strain law in compression depended only on the coefficient FLD. Moreover, they realized that in the case of buckled bar, the softening branch is characterized by a constant ratio between the average stress and strain, equal to 2% of the Young modulus. Finally, average stress approaches a constant value equal to 0.2 f_y, after that a certain value of strain is reached.

On the basis of these considerations, researchers proposed an analytical form of the stress-strain law of reinforcing steel in compression (Fig. 1).

First branch after yielding is defined with a maximum strain equal to ε^*. The corresponding stress σ^* is calculated on the basis of the value σ_l^* recorded in the local stress-strain law of steel, on the basis of the following expressions

$$\frac{\varepsilon^*}{\varepsilon_y} = 55 - 2.3\sqrt{\frac{f_y}{100}\frac{L}{d_b}} \geq 7 \tag{3}$$

$$\frac{\sigma^*}{\sigma_l^*} = \alpha\left(2.2 - 0.016\sqrt{\frac{f_y}{100}\frac{L}{d_b}}\right) \geq 0.2\,f_y \tag{4}$$

where α is a coefficient which depends on the post-elastic branch of steel. Dhakal and Maekawa (2002) suggests α to be equal to 0.75 for perfect plastic and 1 for hardening behaviour.

After the definition of σ^* and σ_l^*, the trend of the stress-strain law in the post-elastic range is defined by the following law

$$\frac{\sigma_s}{\sigma_l} = \left(1 - \left(1 - \frac{\sigma^*}{\sigma_l^*}\right)\left(\frac{\varepsilon - \varepsilon_y}{\varepsilon^* - \varepsilon_y}\right)\right) \geq 0.2 f_y \quad \text{for } \varepsilon_y < \varepsilon < \varepsilon^* \tag{5a}$$

$$\sigma^* - 0.002 E_s \left(\varepsilon - \varepsilon^*\right) \geq 0.2 f_y \quad \text{for } \varepsilon > \varepsilon^* \tag{5b}$$

The main shortcoming of this model is that it requires the definition of the stress-strain law in three branches, and the preliminary calculation of ε^* and σ^*. By contrast, its main advantage is that stress-strain law is represented by linear branches, easy to be integrated and consequently it could be useful for direct integration in sectional analysis.

2.2 Model of Urmson and Mander (2012)

Urmson and Mander (2012) developed a computational fiber element analysis to compute the coupled effect of axial compression and lateral buckling for the case of local buckling.

The results of the analysis were adopted to formulate a simple model for the compressive behavior of reinforcing steel in compression, expressed by the following equation

$$f_s = \frac{E_s \varepsilon_s}{\left(1 + \left|\frac{\varepsilon_s}{\varepsilon_y}\right|^{20}\right)^{0.05} + \left(\frac{0.008}{\varepsilon_y}\right)\left[\left(1 + \left|\frac{\varepsilon_s}{2\varepsilon_{cr}}\right|^{40}\right)^{0.05} - 1\right]} + \left(f_{cr} - f_y\right)\left[1 - \frac{\left|\varepsilon_{cr} - \varepsilon_s\right|^p}{\left[\left|\varepsilon_{cr} - \varepsilon_s\right|^{20p} + \left|\varepsilon_{cr} - \varepsilon_s\right|^{20p}\right]^{0.05}}\right] \tag{6}$$

where

ε_{sh} is the strain at onset of hardening, and it is defined as $\varepsilon_{sh}=8*\varepsilon_y$

E_{sh} is the hardening modulus

f_{su} is the ultimate stress and ε_{su} the ultimate strain defined as $\varepsilon_{su}=40*\varepsilon_y$

f_{cr} is the ultimate compressive (crippling) stress, and ε_{cr} the corresponding strain.

These last two parameters were proposed depending on the ratio between the stirrup's pitch s and the diameter of the bar d_b, as follows

$$f_{cr} = f_{su}\left(1 + \varepsilon_{su}\right)^2 \left[\sqrt{1 + \frac{\left(\frac{s}{d_b}\right)^4}{121}\varepsilon_{su}^2} - \frac{\left(\frac{s}{d_b}\right)^2}{11}\varepsilon_{su}\right] \tag{7}$$

$$\varepsilon_{cr} = \frac{0.014\varepsilon_y^{0.075} + 11 \cdot 10^{-6}}{\left(\frac{s}{d_b}\right)^2 \varepsilon_y^{1.5}} \tag{8}$$

Finally, the exponent p is calculated as

$$p = E_{sh}\frac{\left(\varepsilon_{cr} - \varepsilon_{sh}\right)}{f_{cr} - f_y} \tag{9}$$

Fig. 2 shows the comparison between results achieved by the two models in terms of engineered stress-strain law in compression, for a steel with strain hardening behaviour. Values in the two axis are normalized with respect to the corresponding yield quantities. Moreover, six different values of FLD are considered, ranging from 10 to 20. This comparison allows to clarify the reliability of these analytical formulations, and it shows the variability of possible results achievable with these models available in the literature. It is observed as the difference in the two models' response increases with the increase of the FLD coefficient. Low differences of estimated stress to assigned axial strain are recorded for FLD lower than 14, while the spread increases for very slender bars. It is evident as the two models are not in accordance, since they show similar results only when buckling effects are not evident.

The dependence of each model's accuracy on the FLD coefficient is more evident by Fig. 3, which shows the average ratio between stress estimated by the model of Dhakal and Maekawa σ_{DM}, and that predicted by the model of Urmson and Mander σ_{UM}, as a function of FLD. For the calculation of this ratio, stress was evaluated in 40 points along the post-elastic branch.

In general, the model of Dhakal and Maekawa (2002) provides lower stresses with respect to the model of Urmson and Mander (2012). It is clear to observe that the average difference is negligible (<10%) for FLD≤14, while it increases for slender bars up to a maximum spread of about 38% for FLD=20.

3. Finite element investigation

Reliability analysis of above mentioned analytical models is here performed by means of non-linear finite element analyses carried out with ATENA3D (Cervenka 2016), which is a commonly used code in research for modelling concrete and steel members (Le Hoang and Fehling 2017) due to its capabilities in considering geometrical and mechanical non-linearities. In the following the principles of analysis and the details of the model under study are discussed.

3.1 Model under study

The steel bar was modeled with 3D isoparametric solid elements (CCIsoBrick) with 20 nodes and 20 integration points with hourglass control (Fig. 4). To eliminate shear-locking deficiency, enough elements were provided per thickness in bending direction. The effect of concrete core is accounted by restraining the bar laterally in one way, so the bar can buckle only over a side. Rotations are restrained at both bar's extremities by means of two rigid rectangular blocks, in order to reproduce the condition of clamped end member, consistent with modelling assumed in Dhakal and Maekawa (2002), Urmson and Mander (2012). Additionally, an initial imperfection was imposed to the bar in order to capture the buckling phenomenon. The imperfection was represented by an initial deformed shape with maximum deflection δ_0 equal to $0.1d_b$, according to indications given in Massone and Moroder (2009). Displacement controlled analyses were carried out by

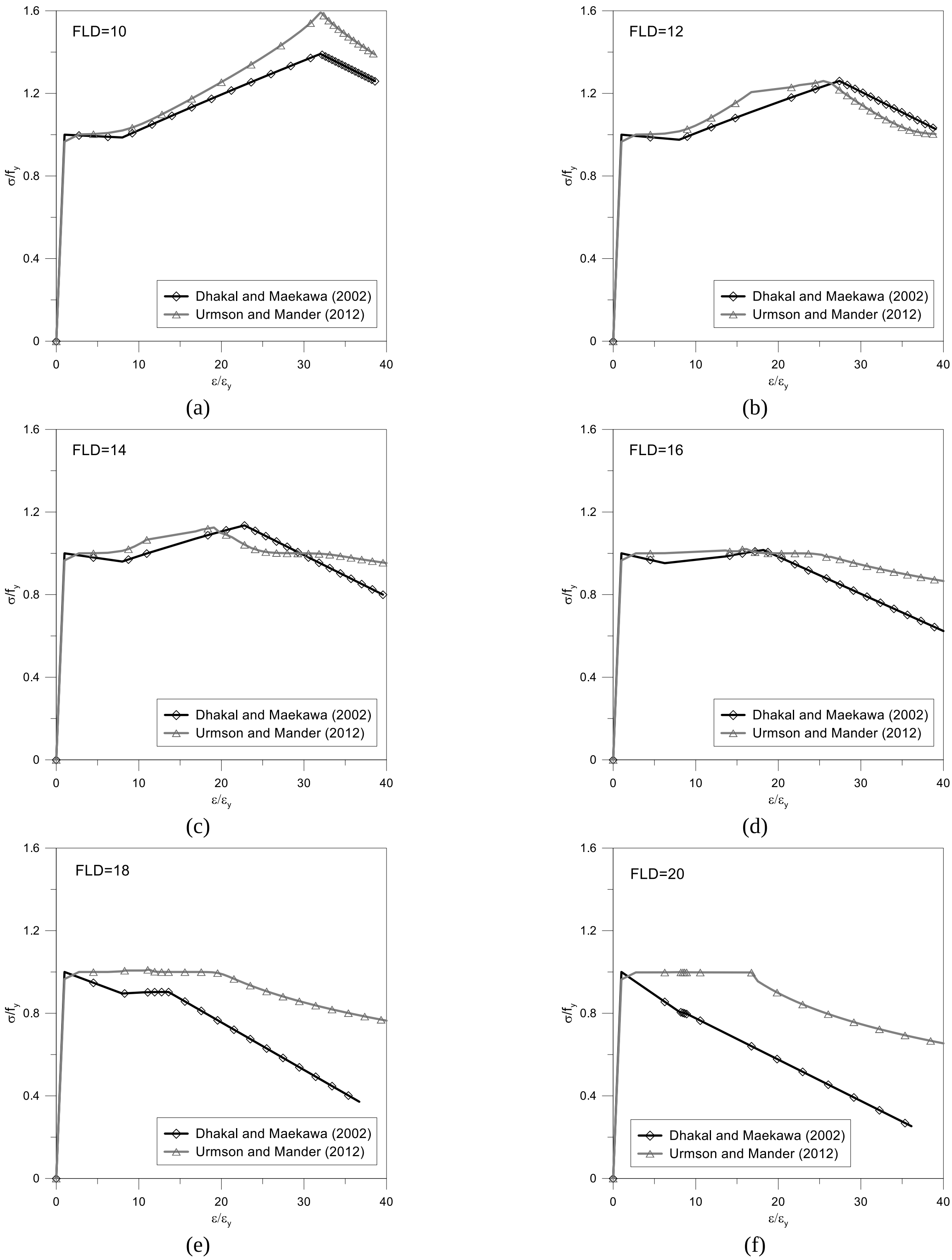

Fig. 2 Comparison between the analytical models' predictions. (a) FLD=10; (b) FLD=12; (c) FLD=14; (d) FLD=16; (e) FLD=18; (f) FLD=20

applying a constant shortening value of 0.03 mm for each step and analysis was interrupted when engineering axial strain was equal to $40\varepsilon_y$. This last assumption means that performed analysis involves large inelastic strains, and consequently the engineering uniaxial constitutive law of steel needs to be converted to a true-stress-true-strain curve. This conversion from engineering to true values can be made by the following relations (Dodd and Restrepo 1995)

$$\sigma_{true} = \sigma_{eng}(1+\varepsilon_{eng}) \tag{10a}$$

$$\varepsilon_{true} = \ln(1+\varepsilon_{eng}) \tag{10b}$$

The definition of an uniaxial stress-strain law is generally suitable to define the isotropic flow stress (yield

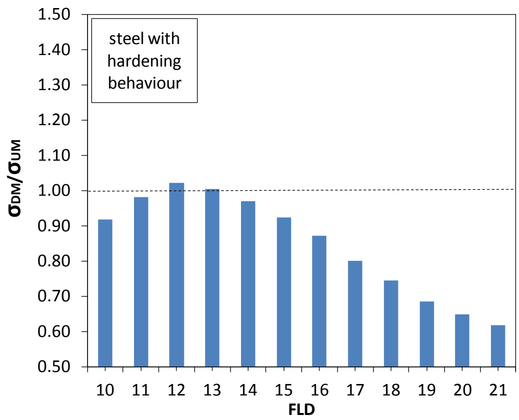

Fig. 3 Average stress error between the model of Dhakal and Maekawa (2002) and Urmson and Mander (2012)

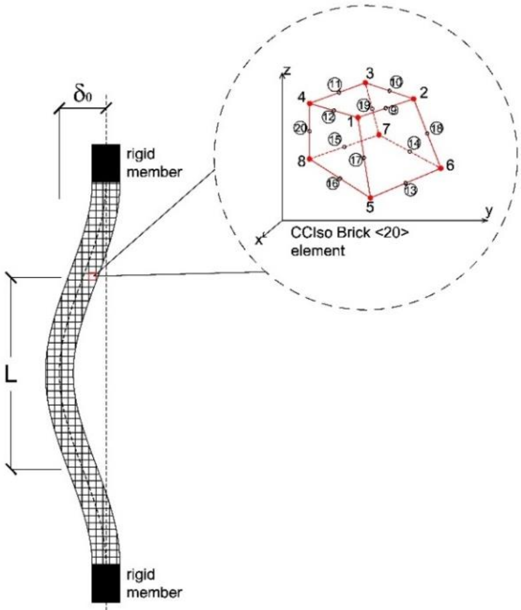

Fig. 4 Schematic representation of the model under study

surface) for structural steel in 3D FE models (Abed *et al*. 2013), and as well known in the literature (Rice 1975) isotropic hardening can be assumed for problems in which the plastic strains overcomes substantially the incipient yield state, neglecting the Bauschinger effect. Consequently, isotropic hardening is here assumed due to the hypothesis of monotonic loading - i.e., the plastic strain rate does not continuously reverse direction sharply and Bauschinger effect is negligible. The adopted material model includes plasticity by means of a yielding function depending only on the second stress invariant J_2, and on the function k which control the hardening of the law.

In this model, the yield function is defined as

$$F^P\left(\sigma_{ij}\right)=\sqrt{J_2}-k\left(\varepsilon_{eq}^p\right)=0 \tag{11}$$

where J_2 is the second stress invariant. Parameter k is the maximum shear stress, calculated as

$$k\left(\varepsilon_{eq}^p\right)=\sqrt{\frac{1}{3}}\sigma_y\left(\varepsilon_{eq}^p\right) \tag{12}$$

Table 1 Mechanical properties of steel in performed analyses

	f_y (MPa)	f_{su} (MPa)	E_s (MPa)	E_{sh} (MPa)	ν	ε_{sh}	ε_{su}
Elastoplastic	550	550	200000	0	0.3	0	$40\varepsilon_y$
Hardening	550	715	200000	4000	0.3	$2\varepsilon_y$	$40\varepsilon_y$

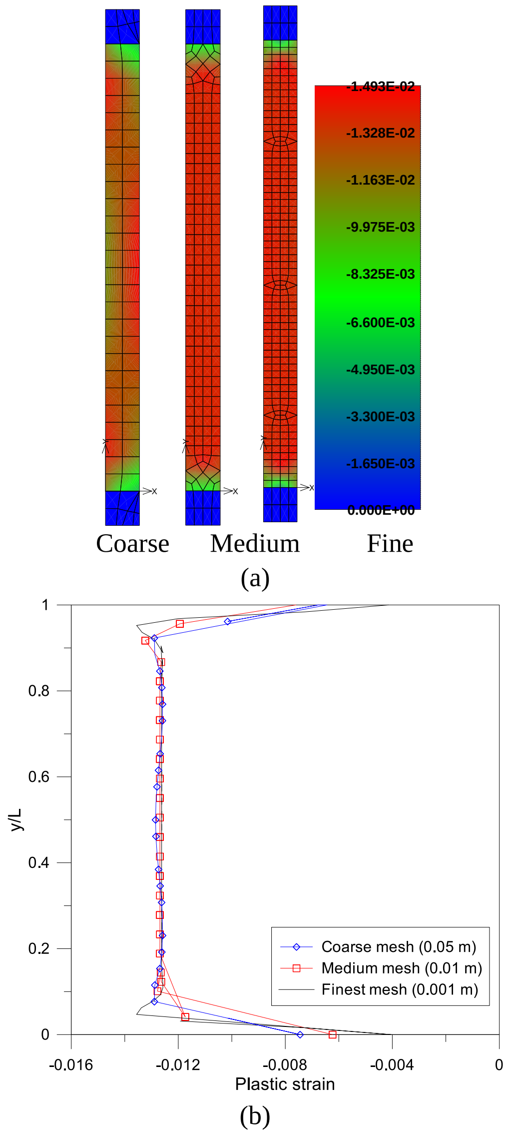

Fig. 5 Mesh sensitivity test of the model FLD=13 (a) Colorplot of plastic strains; (b)Trend of plastic strains along the bar (*x/D*=0.5)

and f_y is the uniaxial yield stress. This parameter rules the isotropic hardening criteria of the yield function

$$\sigma_y\left(\varepsilon_{eq}^p\right)=f_y+E_{sh}\varepsilon_{eq}^p \qquad \varepsilon_{eq}^p=\sum_{i=1}^{N_{imc}}\sqrt{\frac{2}{3}\left(\Delta\varepsilon^p:\Delta\varepsilon^p\right)} \tag{13}$$

being E_{sh} the hardening modulus and ε_{ep} the equivalent plastic strain.

Table 1 shows the main properties adopted for the analyses, for steel with elastoplastic or hardening behaviour. The adopted values are chosen as common material properties for reinforcing bars adopted in Europe.

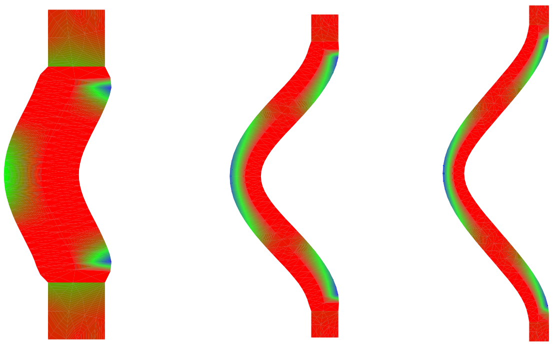

(a) (b) (c)

Fig. 6 Deformed shapes and principal tensile stresses [Units in MPa] (a) FLD=10, (b) FLD=15, (c) FLD=20

Geometrical non-linearity is included by considering the equilibrium of the deformed geometry even during each iteration. Solution was allowed by Newton-Raphson method. This algorithm was chosen since it allowed a stable solution instead of Arc-Length method, which proved to be slower to convergence and less stable.

3.2 Calibration of the mesh

A preliminary test on mesh sensitivity was performed in order to check the reliability of performed analysis. In particular, several models were generated by scaling the mesh size until similar results were obtained in terms of plastic strains. As an example, Fig. 5 shows the results of the mesh sensitivity test on the model of bar with FLD=13, in terms of color plot of plastic strains ε_{py} on the model (Fig. 5(a)) for the same load step and along nodes with the same abscissa x/d_b=0.5, being x/d_b=0 the abscissa corresponding to the bar's edge (Fig. 5(b)). It is worth noting that in this case plastic zone of models with finer mesh tends to be wider than that recorded in models with a coarse mesh. Additionally, when the mesh size is wider the distribution of plastic strains is less uniform with respect to refined models. As a consequence, non refined models are more subjected to strain localization and causes a different trend of the engineering stress-strain curve - not here shown for the sake of conciseness. Therefore, mesh was refined until the engineering stress-strain response was unaltered and the plastic length remains almost unchanged.

3.3 Results

Analyses were performed on different bar's models, by varying the FLD parameter from 10 to 20 and recording the reactions at the bar's ends. These values were adopted since these are in the range of interest for practical cases. Three-hinge mechanism was observed in all models, independently by the bar's slenderness. Fig. 6 shows the deformed shape of the buckled bar with the colorplot of principal tensile strains for three different models, highlighting the mechanism with three plastic hinges.

Fig. 7 shows results in terms of normalized stress-strain response in compression for steel with strain hardening (Fig. 7(a)) or with elastoplastic behaviour (Fig. 7(b)). It is

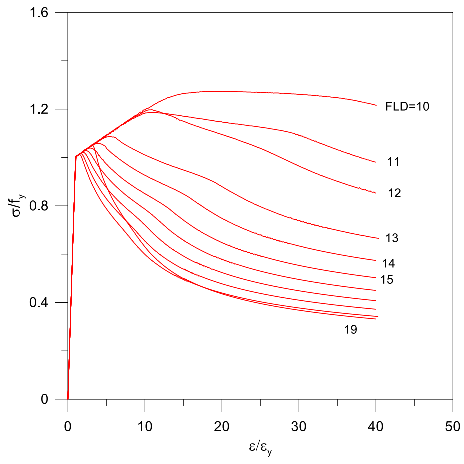

(a)

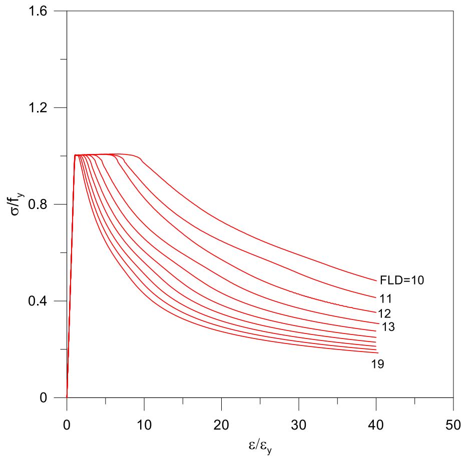

(b)

Fig. 7 Normalised stress-strain response in compression (ATENA FEM) for 10<FLD<20 (a) Hardening behaviour; (b) Elastoplastic behaviour

evident that hardening steel bars are more sensitive to the FLD parameter. This is probably due to the fact that hardening steel has some strength resources after yielding and consequently the decreasing branch is more evident after plastic buckling is activated. Crippling strain -i.e., the axial strain corresponding to the start of the descending branch- is a function of FLD and all models tend to a constant value of residual stress, equal to 0.3f_y for hardening steel and 0.2 f_y for elastoplastic steel.

Fig. 8 shows the trend of the crippling strain ε*, normalized with respect to the yield strain ε_y, as a function of the FLD ratio, for steel with strain hardening. Moreover, Eq. (3) proposed by Dhakal and Maekawa (2002) is plotted for comparison purposes. It is worth to note that substantially lower values of crippling strain are predicted by the current simulations, and the trend is substantially far to be linear, as in Eq. (3). On the basis of performed simulations, ε* decreases as a non-linear function with respect to FLD, and the trend can be approximated by the following expression

$$\frac{\varepsilon^*}{\varepsilon_y} = 68477\left(\frac{L}{d_b}\sqrt{f_y/100}\right)^{-3.659} \tag{14}$$

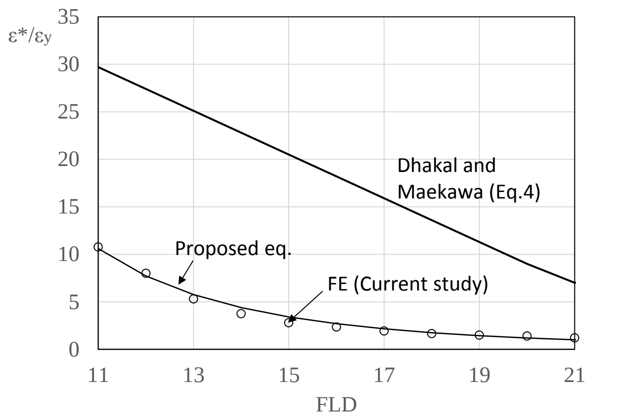

Fig. 8 Normalised crippling strain as a function of FLD (Hardening steel)

Table 2 Mechanical properties of steel in experimental works

	Material	f_y (MPa)	f_{su} (MPa)	E_s (MPa)	E_{sh} (MPa)	ε_{sh}	ε_{su}
Mander *et al.* (1994)	H.S.	869	1130	221	11030	0.0039	0.063
	Mild	331	565	215	8274	0.0091	0.144
Bayrak and Sheikh(2001)	-	515	690	200	9000	0.0089	0.12

The accuracy of performed analysis was verified against experimental data reported in Mander *et al*. (1994), Bayrak and Sheikh (2001). Mechanical properties of specimens for comparison are summarized in Table 2.

Fig. 9(a)-(e) shows the comparisons between the experimental data and theoretical predictions in terms of normalized compressive stress-strain curve. In particular, Fig. 9(a), (b) and (c) are referred to experimental data of Bayrak and Sheikh (2001), while Fig. 9(d) and (e) makes reference to specimens tested by Mander *et al*. (1994). Curves recorded experimentally are compared with previously described models of Dhakal and Maekawa (2002), Urmson and Mander (2012), and the results of performed FE simulation are also reported in red. It is worth to note that analytical models were able to predict the experimental response only for the data of Bayrak and Sheikh (2001), corresponding to pitch-to-diameter ratios equal to 5, 6 and 7. For larger bar's slenderness (8, 9), good accordance is observed only between experimental results and FE simulations. These last in some cases slightly overestimate the stress after the elastic stage, due to the uncertainties in setting a correct value for the strain at the onset of hardening.

Generally, good accuracy is achieved by the performed

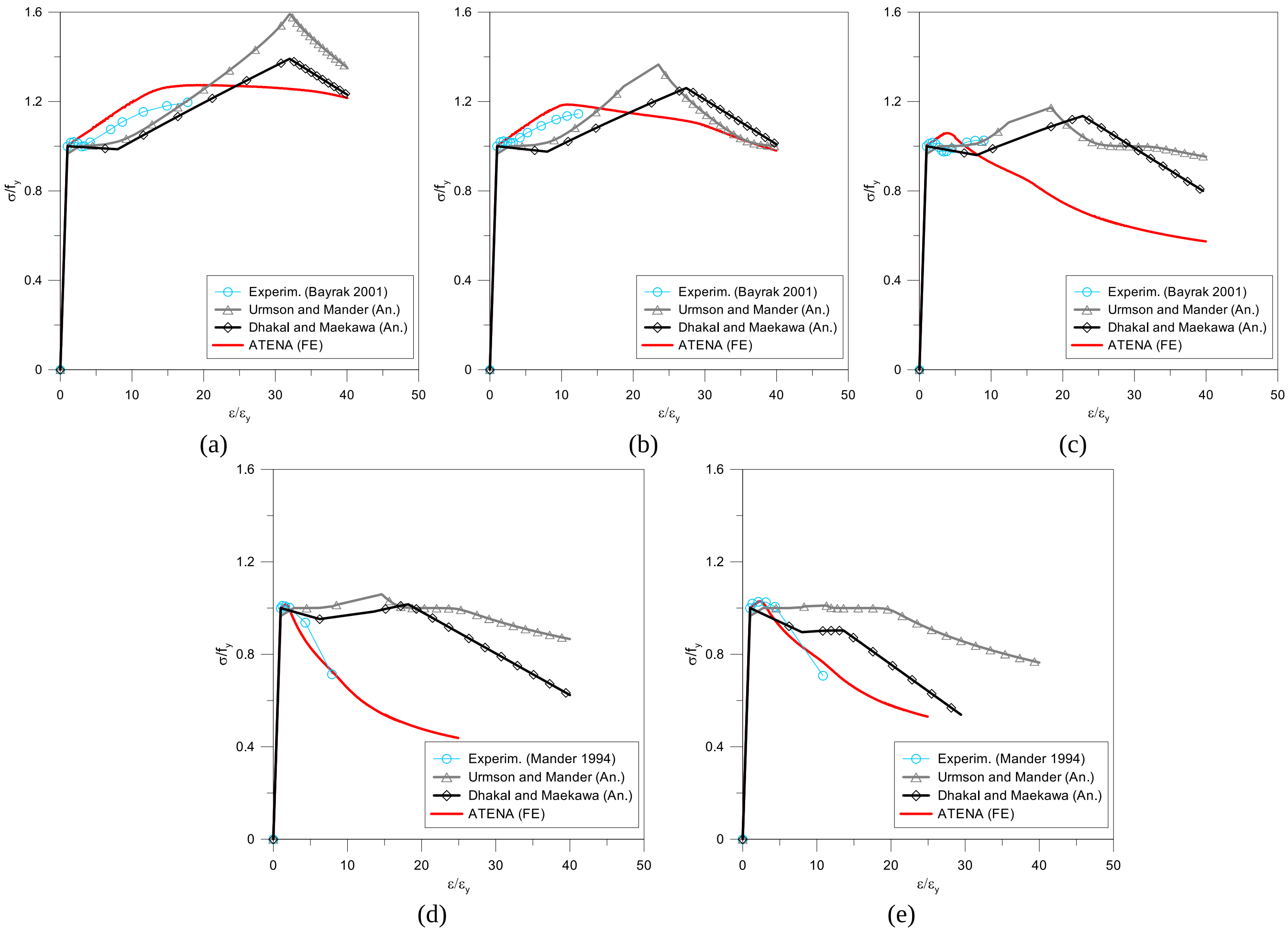

Fig. 9 Comparisons between theoretical predictions and experimental results (a) L/d_b=5; (b) L/d_b=6; (c) L/d_b=7; (Bayrak and Sheik 2001) (d) *L/db*=8 (Mild steel); (e) *L/db*=9 (High strength steel) (Mander *et al*. 1994)

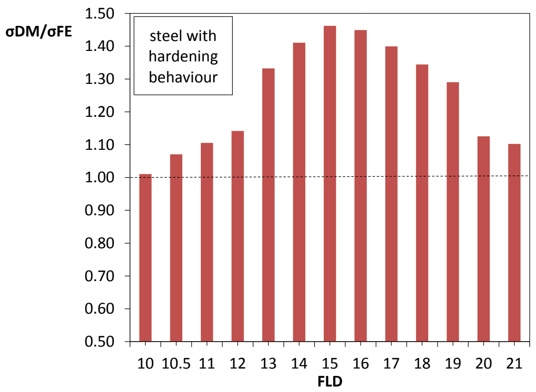

(a)

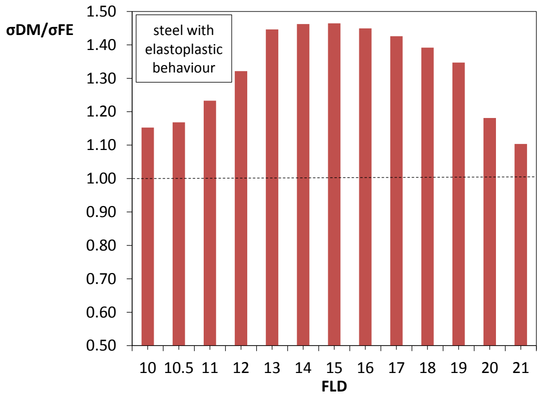

(b)

Fig. 10 Average stress error ratio between DM model and FE analysis. (a) Steel with strain hardening; (b) Steel with elastoplastic behaviour

simulations, able to predict the compressive response of the bar in compression under the assumption of local buckling. Moreover, it is stressed as a wider calibration of analytical models on the basis of FE results is necessary.

In particular, it should be noted that the expressions proposed by Dhakal and Maekawa (2002) (Eq. (3)-(5)) depend on coefficient α, equal to 0.75 for elastoplastic steel and 1 for hardening behaviour. However, since the definition of this parameter substantially affect the trend of the function, it can be calibrated for minimizing the error between the analytical response and FE simulations.

This consideration is more clear by observing the average stress error ratio reported in Fig. 10. In particular, it plots the average difference between engineered stress in the post elastic range predicted by the model of Dhakal and Maekawa (2002) σ_{DM} and that recorded by the FE simulation σ_{FE}.

Fig. 10(a) shows the error bars for steel with strain hardening behaviour and it shows as the average stress error ratio among the examined range of FLD is equal to 1.25 with a Coefficient of Variation (COV) equal to 13%. Similarly, Fig. 10(b) highlights the same error ratio for elastoplastic steel, which value averaged for all examined cases of FLD is equal to 1.32 and COV equal to 10%. In both cases, maximum errors are achieved for a value of FLD equal to 15, which is a value of practical interest as it corresponds to a L/d_b ratio equal to 7.5 for a bar with f_y=400 MPa. It should be also noted that s/d_b ratio equal to 8 corresponds to the code recommendation of Eurocode 8 for maximum value of stirrup's pitch. In this case, the analytical model of Dhakal and Maekawa (2002) tends to overestimate the response obtained by FE analysis of about 45%. Moreover, the application of the analytical model leads to greater errors for elastoplastic steel. In addition, this case is of interest with respect to strain hardening behaviour, due to the fact that perfectly plastic behaviour is a common assumption in compressive constitutive relationships adopted for steel rebars. Results for the model of Urmson and Mander (2012) gave greater errors, with a similar trend to that observed for the model of Dhakal and Maekawa (2002). Results are not reported for the sake of brevity.

4. Proposed modification to the model of Dhakal and Maekawa (2002)

On the basis of the comparison between FE analysis results and the application of the model of Dhakal and Maekawa (2002), a modification of this last model was studied in order to fit numerical results.

Error regression analysis was performed by comparing the results of analytical model of Dhakal and Maekawa (2002) and FE simulations. It was observed that when the local stress-strain law of steel included a strain hardening behaviour, the difference between the two approaches increased significantly when FLD ratio was in the range between 13 and 20, as observed in Fig. 10(a). Differently, outside of this range the error was lower than 10%. As a consequence, focus was made in this examined range and the value of the coefficient α was search to minimize the average error. Summarizing the results for hardening steel, proposed coefficient α is

$$\text{for FLD}<13 \quad \alpha=1; \tag{15a}$$

$$\text{for } 13 \le \text{FLD} \le 19 \quad \alpha=0.75; \tag{15b}$$

$$\text{for FLD}>19 \quad \alpha=1; \tag{15c}$$

Fig. 11 shows the comparisons between results achieved by the FE simulations and those obtained by the analytical model of Dhakal and Maekawa (2002) with or without the proposed modification to the coefficient α. Three cases are shown corresponding to FLD equal to 13, 15 and 19 in Fig. 11(a), (b) and (c) respectively. It is evident that the accordance between the analytical expression and the numerical solution is noticeably improved. The original model tends to overestimate the response, as observed above, while proposed modification allows obtaining an engineered stress-strain relationship more consistent with non-linear FE simulations.

A similar modification was also studied for steel with local stress-strain relationship idealized as elastic perfectly plastic. In this case, it was observed that greater differences between the analytical solution and the FE results are expected for all the range of FLD values (10≤FLD≤20, Fig. 10(b)). In this case, the modification to the coefficient α required the solution of an optimization problem. Very

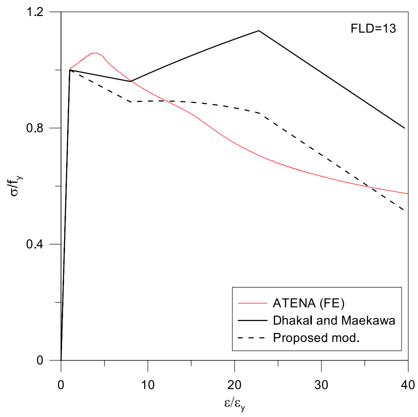

(a)

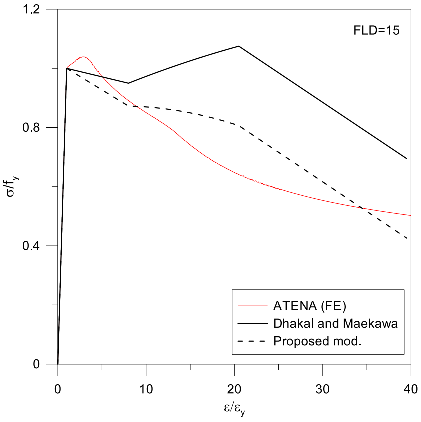

(b)

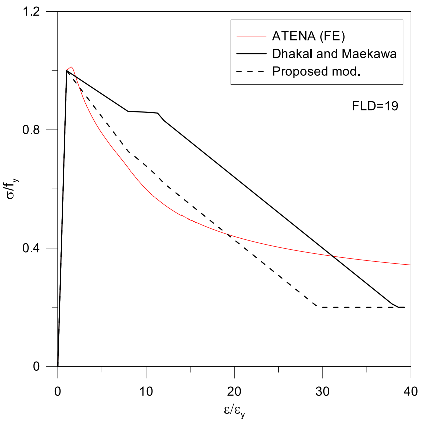

(c)

Fig. 11 Proposed model for hardening steel (a) FLD=13; (b) FLD=15; (c) FLD=19

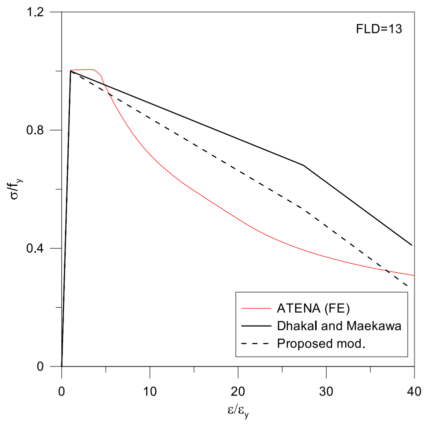

(a)

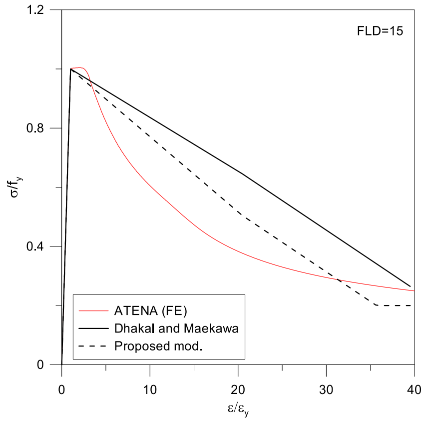

(b)

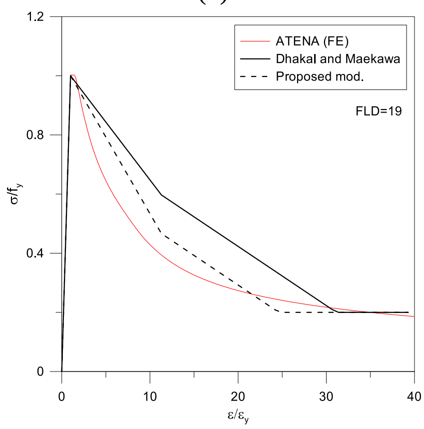

(c)

Fig. 12 Proposed model for elastoplastic steel (a)FLD= 13; (b) FLD=15; (c) FLD=19

different values of α were obtained for each case for minimizing the average stress error and a line search optimization procedure was set to find the value of α which minimizes error and COV. As a result, the following values are proposed for elastoplastic steel

$$\text{for FLD<10} \quad \alpha=0.75; \tag{16a}$$

$$\text{for } 10 \le \text{FLD} \le 20 \quad \alpha=0.586; \tag{16b}$$

$$\text{for FLD>20} \quad \alpha=0.75; \tag{16c}$$

Fig. 12 shows some examples of application of proposed modification for elastoplastic steel. The same cases of FLD parameter are considered with respect to the case of strain hardening steel. The proposed model slightly overestimates the FE response, with a maximum difference of 13%. In general, also in this case, proposed modification to the coefficient allows improving the accordance between results of FE simulations and a closed form expression.

The performance of the proposed model in the overall examined range of FLD is shown in Fig. 13, which plots the error bars, giving the average ratio between stress predicted by the proposed model σ_{PR} and that obtained by the FE simulations $\sigma_{FE.}$ It is observed that for the case of steel with local hardening behaviour (Fig. 13(a)) the average ratio

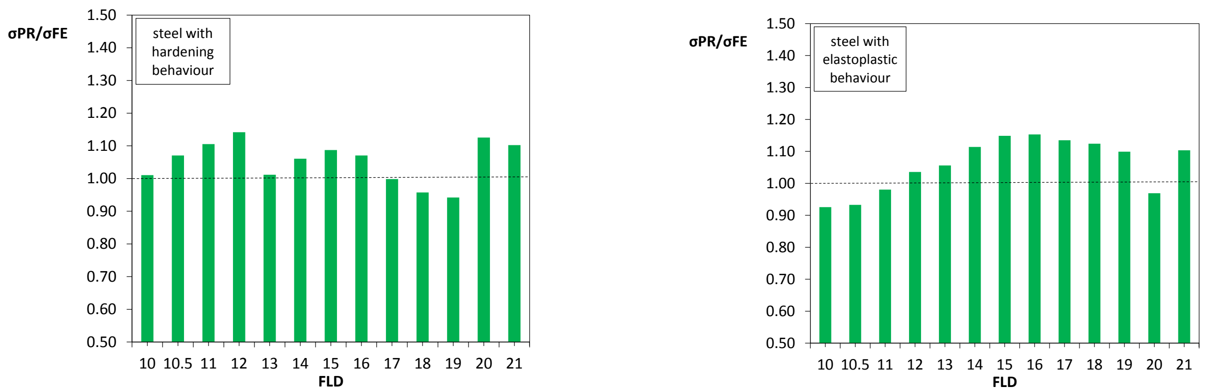

(a) (b)

Fig. 13 Average stress error ratio between proposed model and FE analysis. (a) Steel with hardening; (b) Steel with elastoplastic behaviour

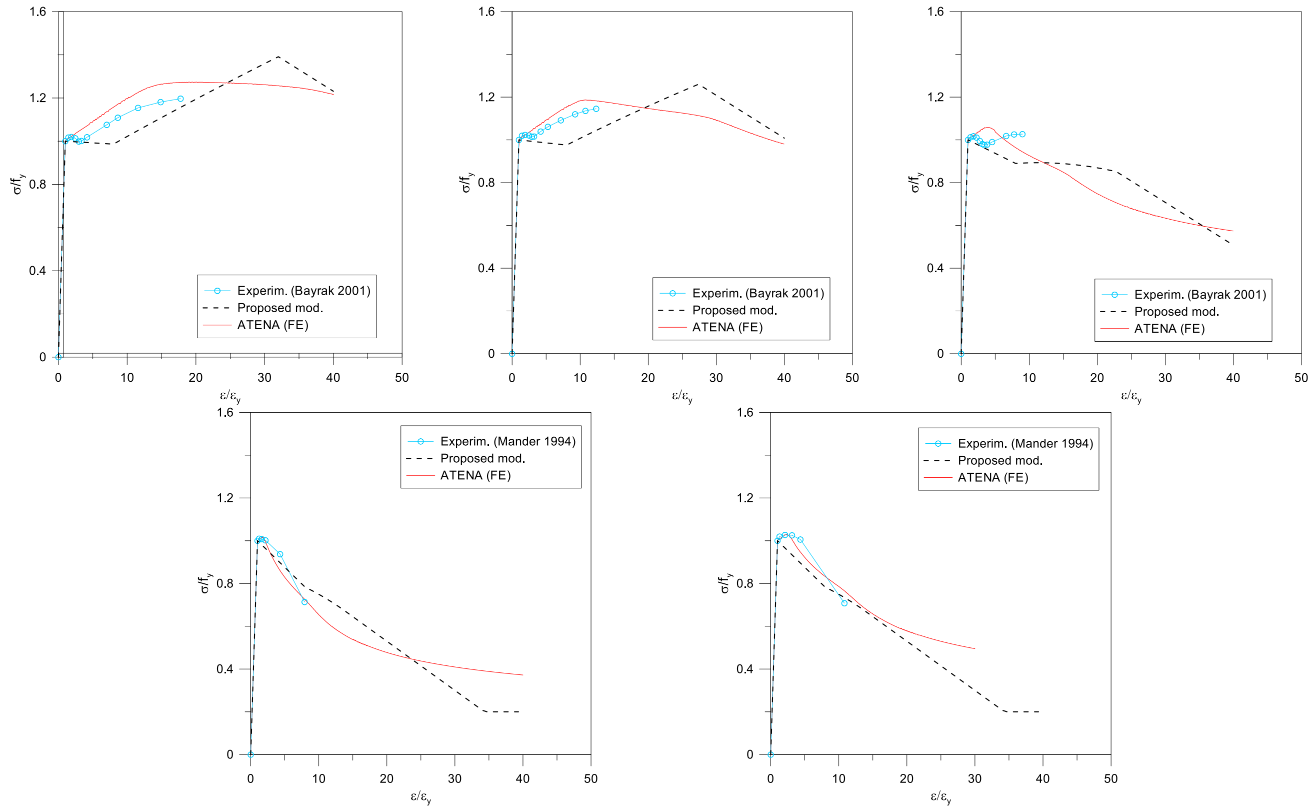

Fig. 14 Comparison between proposed model, numerical simulations and experimental results

$(\sigma_{PR}/\sigma_{FE})_{AV}$ for the overall range is equal to 1.05 and COV is equal to 6%. Similarly, for elastoplastic steel $(\sigma_{PR}/\sigma_{FE})_{AV}$ is equal to 0.92 and COV is 3.3%. It is evident that a substantial improvement is obtained with respect to the cases of Fig. 10.

Finally, theoretical predictions achieved with proposed model are compared with experimental results, as shown in Fig. 14. It is worth to note that FLD values are equal to 16 and 18 for tests of Mander (1994), while they are equal to 10, 12 and 14 for results of Bayrak and Sheik (2001). In other words, the model is validated among the entire range of FLD. The analytical prediction allows following both the numerical and experimental results with a good accuracy for each case examined.

5. Example of application

In this section an example of application of the proposed model is shown, describing how the proposed constitutive law of steel in compression can be adopted for predicting the compressive behaviour of axially loaded RC columns. Reference is made to the specimen CS8 tested in Razvi and Saatcioglu (1999), which is an high strength concrete (HSC) column with square cross section having side 218.7 mm, reinforced with eight longitudinal bars with diameter equal to d_b=11.3 mm and stirrups -diameter 11.3 mm- placed at pitch L=85 mm. The compressive strength of unconfined concrete is equal to 105.4 MPa, while the yield stress of longitudinal bars is f_y=400 MPa.

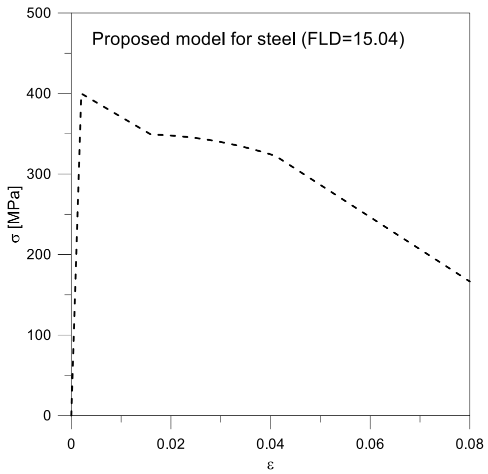

(a)

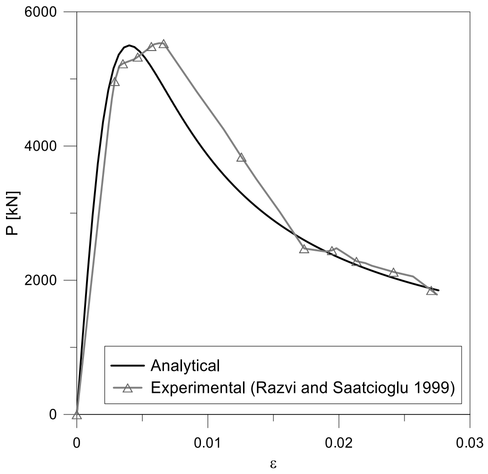

(b)

Fig. 15 Application of proposed model for predicting the compressive behaviour of Specimen CS8 tested in Razvi and Saatcioglu (1999). (a) Proposed model for steel in compression; (b) Axial load-strain curve

On the basis of these features, the FLD coefficient for longitudinal bars is equal to 15.04 (Eq. (2)), and the compressive behaviour of longitudinal steel bars is defined by Eqs. (3)-(5), being the proposed coefficient α equal to 0.586 according to Eq. (15b). The stress-strain law of longitudinal bars is plotted in Fig. 15(a), and it shows that second order effects are not negligible. Finally, the axial load-strain of the column is calculated by adding the contribution of the concrete, this last is calculated by adopting the model proposed in Campione and Minafò (2010) for HSC columns. Fig. 15(b) plots the comparison between the analytical response and with experimental data in terms of axial load-strain curve. Good accordance is noted between the analytical solution and the experimental response, showing that the proposed model can be successfully adopted for predicting the compressive behaviour of RC members.

On the basis of the comparison between FE analysis results and the application of the model of Dhakal and Maekawa (2002), a modification of this last model was studied in order to fit numerical results.

6. Conclusions

This paper presented a numerical investigation on the compressive response of steel rebars. The target of the work was to assess the reliability of existing closed-form analytical expression for predicting the engineered stress-strain law under monotonic compression, including buckling effects. It was shown that existing literature models of Dhakal and Maekawa (2002), Urmson and Mander (2012) give different results depending on the value of the coefficient FLD. 3D non-linear FE simulations were performed to calibrate a constitutive law in an analytic form. From performed analyses and for the range of considered variables, the following conclusions can be drawn:

- the difference of results between FE simulations and existing literature models depends mainly on the value of FLD and on the hypothesis of local hardening or elastoplastic behaviour. Good predictions by the model of Dhakal and Maekawa (2002) are obtained for hardening steel and for FLD<13 or FLD>19. Contrarily, greater errors in all other cases, with maximum spreads for FLD≅15-16 and elastoplastic steel;
- Numerical analyses stressed the need for a wide calibration of an analytical model. In fact, performed simulations with 3D finite elements allow good agreement with experimental results available in the literature, differently from the application of analytical models;
- A modification of the law of Dhakal and Maekawa (2002) was proposed, by changing the parameter α, depending on the hypothesis on the local behaviour of steel (elastoplastic or hardening) and on the value of FLD. This modification allows a good reliability in predicting results achieved by non-linear FE analyses and its accuracy was also tested against experimental data available in works of Mander (1994), Bayrak and Sheik (2001).

References

Bayrak, O. and Sheikh, S.A. (2001), “Plastic hinge analysis”, *J. Struct. Eng*., **127**(9), 1092-1100.

Bechtoula, H., Sakashita, M., Kono, S. and Watanabe, F. (2005), “Seismic performance of 1/4-scale RC frames subjected to axial and cyclic reversed lateral loads”, *Comput Concrete*, **2**(2), 147-164.

Campione, G. and Minafò, G. (2010), “Compressive behavior of short high-strength concrete columns”, *Eng. Struct*., **32**(9), 2755-66.

Can Girgin, S., Moharrami, M. and Koutromanos, I. (2018) “Nonlinear beam-based modeling of RC columns including the effect of reinforcing bar buckling and rupture”, *Earthq. Spectra*, **34**(3), 1289-1309.

Červenka, V. and Červenka, J. (2016), ATENA Program Documentation Part 1- Theory, Prague, Červenka, Consulting s.r.o.

Dhakal, R.P. and Maekawa, K. (2002), “Modeling of post-yield buckling of reinforcement”, *J. Struct. Eng*., ASCE, **128**(9), 1139-1147.

Dodd, L.L. and Restrepo-Posada, J.I. (1995), “Model for predicting cyclic behavior of reinforcing steel”, *J. Struct. Eng.*, ASCE, **121**(3), 433-445.

Gomes, A. and Appleton, J. (1997), “Nonlinear cyclic stress-strain relationship of reinforcing bars including buckling”, *Eng. Struct.*, **19**(10), 822-826.

Kolwankar, S., Kanvinde, A., Kenawy, M. and Kunnath, S. (2017), “Uniaxial monlocal formulation for geometric nonlinearity-induced necking and buckling localization in a steel bar”, *J. Struct. Eng.*, ASCE, **143**(9), 04017091.

Le Hoang, A. and Fehling, E. (2017), “Numerical analysis of circular steel tube confined UHPC stub columns”, *Comput. Concrete*, **19**(3), 263-273.

Mander, J. (1983), “Seismic design of bridge piers”, Ph. D. Thesis, University of Canterbury, Christchurch, New Zealand.

Mander, J.B., Panthaki, F.D. and Kasalanati, A. (1994), “Low-cycle fatigue behavior of reinforcing steel”, *J. Mater. Civil Eng.*, **6**(4), 453-468.

Massone, L.M. and Moroder, D. (2009), “Buckling modeling of reinforcing bars with imperfections”, *J. Struct. Eng.*, **31**(3), 758-767.

Menegotto, M. and Pinto, P. (1973), “Method of analysis for cyclically loaded reinforced concrete plane frames including changes in geometry and non-elastic behavior of elements under combined normal force and bending”, *Proceedings of IABSE Symposium on Resistance and Ultimate Deformability of Structures Acted on by Well Defined Repeated Loads*, International Association for Bridge and Structural Engineering, Zurich, Switzerland.

Minafò, G. and Papia, M. (2017), “Theoretical approaches for modelling buckling effects in rebars of RC members”, *Bull. Earthq. Eng.*, **15**(12), 5309-5327.

Monti, G. and Nuti, C. (1992), “Nonlinear Cyclic Behavior of Reinforcing Bars Including Buckling”, *J. Struct. Eng.*, ASCE, **118**(12), 3268-3284.

OpenSees (Computer software), Pacific Earthquake Engineering Research Center, Univ. of California, Berkeley, CA.

Razvi, S. and Saatcioglu, M. (1999) “Confinement model for high-strength concrete”, *J. Struct. Eng*., ASCE, **125**(3), 281-288.

Rice, J.R. (1975), “Continuum mechanics and thermodynamics of plasticity in relation to microscale deformation mechanisms”, *Constitutive Equations in Plasticity*, Massachusetts Institute of Technology Press, Cambridge.

Shirmohammadi, F. and Esmaeily, A. (2016), “Software for biaxial cyclic analysis of reinforced concrete columns”, *Comput. Concrete*, **17**(3), 353-386.

Urmson, C. and Mander, J. (2012), “Local buckling analysis of longitudinal reinforcing bars”, *J. Struct. Eng.*, ASCE, **138**(1), 62-71.

Yön, B. and Calay, Y. (2014), “Effects of confinement reinforcement and concrete strength on nonlinear behaviour of RC buildings”, *Comput. Concrete*, **14**(3), 279-297.

Zong, Z., Kunnath, S. and Monti, G. (2013), “Simulation of reinforcing bar buckling in circular reinforced concrete columns”, *J. Struct. Eng*., **110**(4), 607-661.

CC